

Structural and optical properties of $\text{SnO}_2\text{-Al}_2\text{O}_3$ nanocomposite synthesized via sol-gel route

NEERAJ K. MISHRA¹, CHAITNAYA KUMAR¹, AMIT KUMAR^{1,2}, MANISH KUMAR^{3,4},
PRATIBHA CHAUDHARY⁵, RAJEEV SINGH^{1,*}

¹Material/Organometallics Laboratory, Department of Chemistry, Atma Ram Sanatan Dharma College, University of Delhi, New Delhi-110 021, India

²Japan Advanced Institute of Science and Technology, 1-1 Asahidai, Nomi City, Ishikawa 923-1292, Japan

³Department of Physics, Atma Ram Sanatan Dharma College, University of Delhi-110 021, India

⁴Materials Research Laboratory, Department of Physics, Banaras Hindu University, Varanasi-221005, India

⁵Department of Chemistry, Maitreyi College, University of Delhi, Bapudham Complex, Chanakyapuri, New Delhi-110 021, India

A nanocomposite of $0.5\text{SnO}_2\text{-}0.5\text{Al}_2\text{O}_3$ has been synthesized using a sol-gel route. Structural and optical properties of the nanocomposite have been discussed in detail. Powder X-ray diffraction and scanning electron microscopy with energy-dispersive X-ray diffraction spectroscopy confirm the phase purity and the particle size of the $0.5\text{SnO}_2\text{-}0.5\text{Al}_2\text{O}_3$ nanocomposite (13 to 15 nm). The scanning electron microscopy also confirms the porosity in the sample, useful in sensing applications. The FT-IR analysis confirms the presence of physical interaction between SnO_2 and Al_2O_3 due to the slight shifting and broadening of characteristic bands. The UV-Vis analysis confirms the semiconducting nature because of direct transition of electrons into the $0.5\text{SnO}_2\text{-}0.5\text{Al}_2\text{O}_3$ nanocomposites.

Keywords: *nanocomposite; sol gel; X-ray diffraction; optical properties*

© Wroclaw University of Technology.

1. Introduction

Semiconducting oxides ZnO , SnO_2 , In_2O_3 and Cd_2SnO_4 have been widely studied because of their great technological importance and novel properties including the structural, optical, electrical [1–4]. These nanomaterials exhibit high electrical conductivity, high optical transmittance in the UV-Vis region and high IR reflectance. Conducting and semiconducting nanomaterials have been widely utilized as an essential part of many optoelectronic devices, such as solar cells and thin film transistors [5, 6]. Tin oxide (SnO_2) and composites of tin oxides are well-known for their structural and optical properties when made into nanoscale and are expected to demonstrate applications, such as solar energy conversion, catalysis, gas sensing, anti-static coating and transparent electrode preparation

[8–13]. The performances of these devices are greatly dependent on the electrical and optical properties of the transparent electrodes and also the method of their preparation [14].

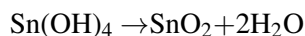
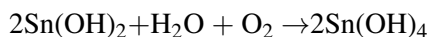
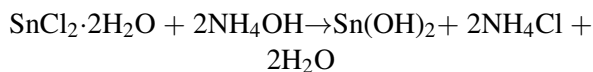
It is well-known that the magnitude of improvement of the structural and optical properties depends strongly on the composition, size and surface area of the nanopowders. Therefore, the composite of a hard nanostructured material, such as Al_2O_3 with SnO_2 matrix looks promising to produce an excellent composite and improve the structural and optical properties of the matrix, such as the size and transparent nature of the material. The composite nanopowders have been synthesized via various methods, such as chemical vapour synthesis, hydrothermal route, inert gas condensation, laser ablation, and sol-gel processing. The sol-gel method is one of the most promising methods because it offers many advantages for synthesizing

*E-mail: rajeev@arsd.du.ac.in

high homogeneity and well-controlled properties of the nanopowders. Excellent control of the stoichiometry of the precursor solution, customizable microstructure, ease of compositional modification, ease of introducing various functional groups of materials, relatively low annealing temperature, and simple and inexpensive equipment are the additional advantages of this process [15]. In the present investigation, it is reported the synthesis of crystalline SnO₂-Al₂O₃ composites by sol-gel route. The main aim of the present research was to gain an understanding of the effect of Al₂O₃ content on the crystallization and phase transformation in the mentioned nanopowders. In addition, it was investigated the influence of the Al₂O₃ content on the size, morphology and optical properties of the composite powders which are determinative factors for particles as reinforcement of the composite matrix.

2. Experimental

Nanocomposites of 0.5SnO₂-0.5Al₂O₃ were prepared at 450 °C by sol-gel route. An ethanolic solution of aluminium trichloride (AlCl₃) (15 mmol) was added to an ethanolic solution of tin dichloride dihydrate (SnCl₂·2H₂O) (15 mmol) under vigorous stirring, which resulted in the formation of a transparent sol. Thereafter, an amount of 7.7 mL aqueous ammonia solution was added dropwise to the above solution under stirring in a controlled manner. The resulting gel was filtered and washed with methanol to remove impurities, and subsequently dried at 100 °C for 2 h in order to obtain a dried gel. The dried gel was further sintered at 450 °C for 4 h to obtain a fine homogeneous dense powder. The condition of oxidation Sn(II) to Sn(IV) is given as:



The phase crystallinity and structural analysis of the 0.5SnO₂-0.5Al₂O₃ nanocomposite was

analyzed by powder X-ray diffraction patterns, recorded using Philips (X'Pert PRO, Model PW 3040) X-ray diffraction system. Surface morphology of 0.5SnO₂-0.5Al₂O₃ was examined by scanning electron microscope (SEM) with EDX (Zeiss EDAX EVO-18 at 15 kV). The optical transmission of the nanocomposite was recorded at room temperature by a dual beam UV-Vis spectrometer (Hitachi-3300) with an integrating sphere in the wave length range of 300 to 900 nm. FT-IR spectra have been recorded on a Nicolet 5700 in transmission mode in the wave number range of 400 to 4000 cm⁻¹. The spectroscopic grade KBr pellets have been used for collecting the spectra with a resolution of 4 cm⁻¹ performing 32 scans. UV-Vis absorption studies were carried out on a Shimadzu 1601 spectrophotometer.

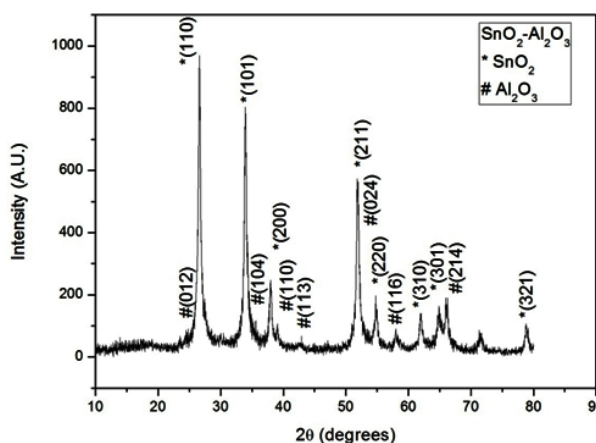


Fig. 1. Powder XRD pattern of SnO₂-Al₂O₃ nanocomposite.

3. Results and discussion

The phase purity of SnO₂-Al₂O₃ nanocomposite was studied by powder X-ray diffraction (XRD) patterns as shown in the Fig. 1. Miller indices (hkl) of the diffraction peaks of SnO₂-Al₂O₃ nanocomposites have been matched with JCPDS Card No. 41-1445 and 46-1212. Powder XRD patterns confirm that there is no appearance of any impurity peaks in the nanocomposite. The peak broadening in the XRD pattern of the SnO₂-Al₂O₃ nanocomposites clearly indicates that the particles are

nanosized with the size ranging between 13 and 15 nm, as confirmed by Debye-Scherrer formula.

Fig. 2 shows the scanning electron micrographs (SEM) of $\text{SnO}_2\text{-Al}_2\text{O}_3$ nanocomposite at different magnifications in the 200 nm range. It is observed from the micrographs that nanocomposite clustering of particles seems to have occurred on the surface. It confirms some nonuniformity in the shapes of the nanoparticles and the existence of porosity, which is useful in sensing applications. The particle size of $\text{SnO}_2\text{-Al}_2\text{O}_3$ nanocomposite measured from SEM images is found to be nearly 62 nm, which is greater as compared to the one calculated from powder XRD. The increment in particle size of the nanocomposite is due to the sintering at 450 °C, resulting in particle binding and agglomeration [7].

Fig. 3 shows energy dispersive X-ray (EDX) spectroscopic analysis of $\text{SnO}_2\text{-Al}_2\text{O}_3$ nanocomposite. It confirms the chemical composition present in the sample. It depicts that aluminium, tin and oxygen elements are present in the nanocomposite, whereas chlorine and gold are also present in trace amounts, which has also been reported in the literature [9]. The component of oxygen (atomic %) is observed to be almost five times that of aluminium and nine times that of tin. Hence, it confirms that the chemical composition should be $\text{SnO}_2\text{-Al}_2\text{O}_3$ and it also agrees with the peaks of SnO_2 and Al_2O_3 in powder XRD spectra.

The FT-IR from 3500 to 659 cm^{-1} for $\text{SnO}_2\text{-Al}_2\text{O}_3$ nanocomposite was studied and the results are shown in Fig. 4. The characteristic broad absorption peak at 3450 cm^{-1} belongs to OH-stretching band vibrations. The peak corresponding to 659 cm^{-1} is assigned to stretching vibration of $\text{V}_{\text{Al-O}}$. However, in case of nanocomposite, a slight shifting and broadening of characteristic bands is observed which indicates the presence of physical interaction between tin and aluminium. The presence of water molecules adsorbed on the surface of SnO_2 during handling or OH groups stretching vibrations can be seen in the regions of 1618 to 1635 cm^{-1} and 3200 to 3600 cm^{-1} [10, 11].

Fig. 5 shows the UV-Vis spectra of $\text{SnO}_2\text{-Al}_2\text{O}_3$ nanocomposite at 450 °C. The

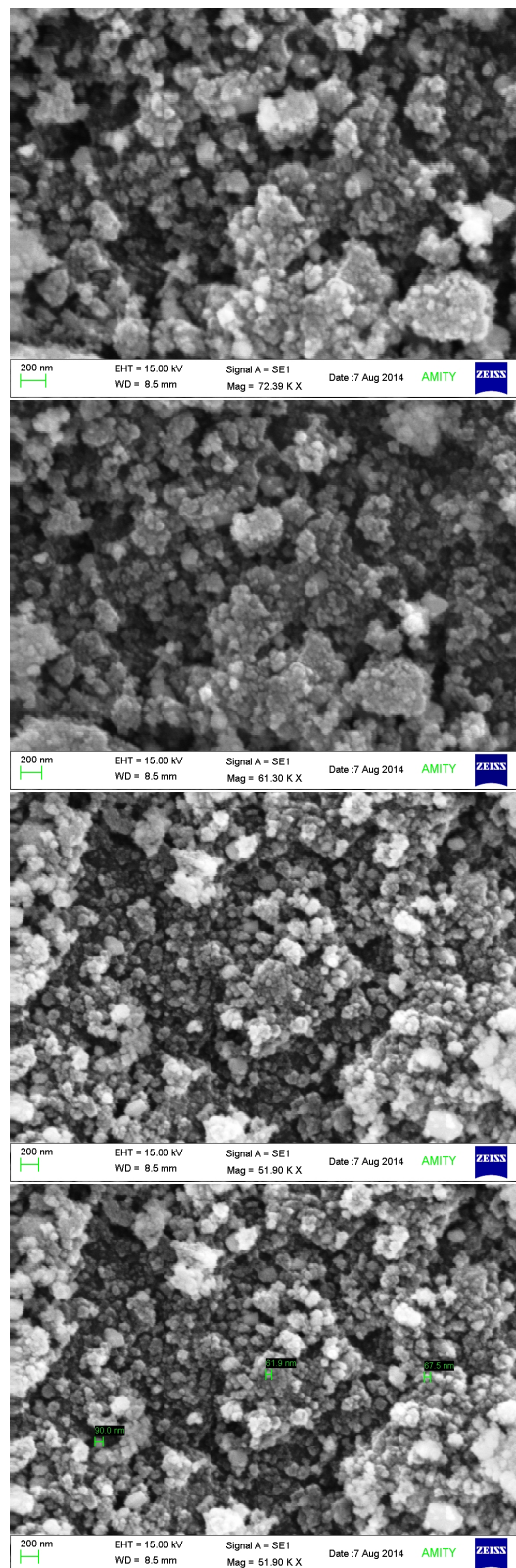


Fig. 2. SEM micrograph of $\text{SnO}_2\text{-Al}_2\text{O}_3$ nanocomposite.

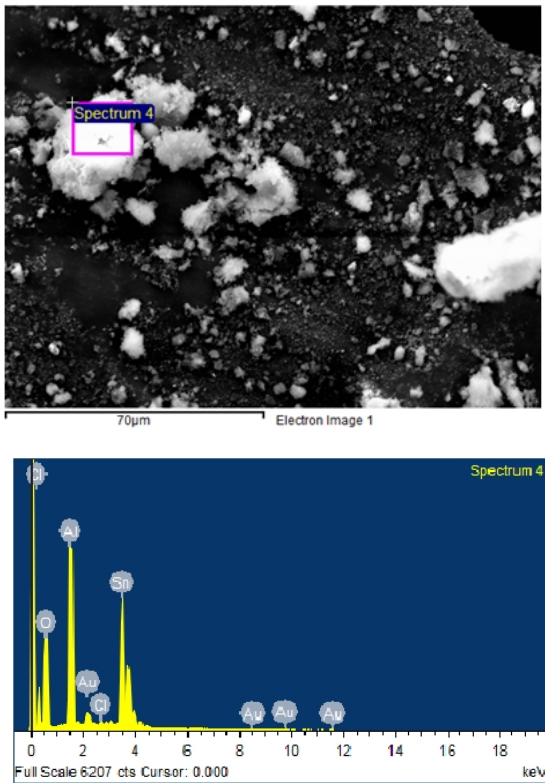


Fig. 3. Energy dispersive X-ray (EDX) spectroscopic analysis of $\text{SnO}_2\text{-Al}_2\text{O}_3$ nanocomposite.

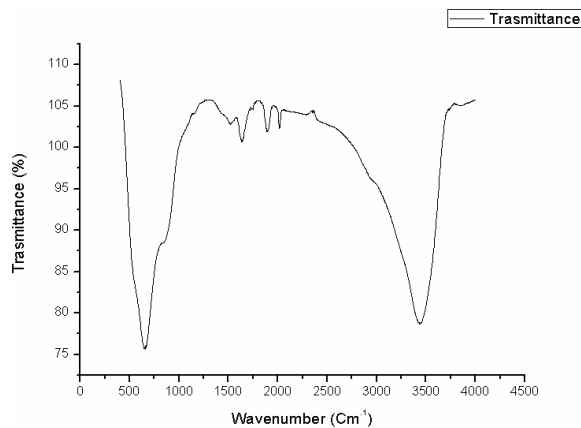


Fig. 4. Infrared spectra of $\text{SnO}_2\text{-Al}_2\text{O}_3$ nanocomposite.

quantum confinement is expected in the semiconductor nanoparticles. It has been found that the absorption edge is shifted to a higher energy when the particle size decreases. It is confirmed by Fig. 5 that the absorption edge of the samples sintered at 450°C is 298 nm. The absorption edge appears

red-shifted to some extent due to the larger particle size of the nanocomposite. Considering the blue shift of the absorption positions from the bulk $\text{SnO}_2\text{-Al}_2\text{O}_3$ composite, the absorption onset of the samples can be assigned to the direct transition of electrons in the $\text{SnO}_2\text{-Al}_2\text{O}_3$ nanocomposites which confirms the semiconducting nature of the sample [16].

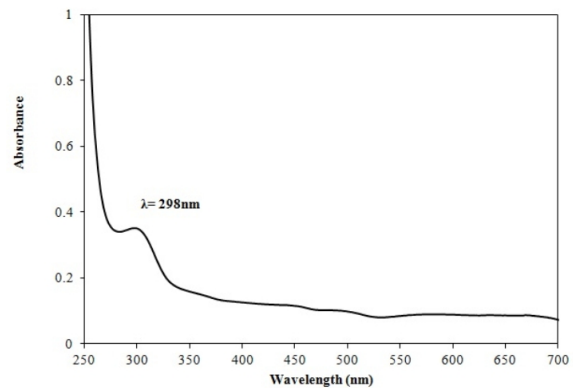


Fig. 5. UV-Vis spectra of the $\text{SnO}_2\text{-Al}_2\text{O}_3$ nanocomposite.

4. Conclusions

In conclusion, $\text{SnO}_2\text{-Al}_2\text{O}_3$ nanocomposite has been successfully synthesized by sol-gel route. The phase purity and the particle size of the $\text{SnO}_2\text{-Al}_2\text{O}_3$ nanocomposite (13 to 15 nm) have been confirmed by the powder XRD. The considerable porosity of the $\text{SnO}_2\text{-Al}_2\text{O}_3$ nanocomposite has been confirmed by SEM, which showed its usefulness in sensing applications. The optical characterizations (FT-IR and UV-Vis) confirmed physical interaction between SnO_2 and Al_2O_3 due to slight shifting and broadening of characteristic bands and the semiconducting nature of the nanocomposite because of direct transition of electrons in the $\text{SnO}_2\text{-Al}_2\text{O}_3$ nanocomposites. To conclude, our results provide the structural, microstructural and optical analysis of the $\text{SnO}_2\text{-Al}_2\text{O}_3$ nanocomposite.

Acknowledgements

The authors are thankful to the University Grant Commission, India, for their support through the Major Research Project F. No. 42-286/2013 (SR).

References

- [1] FANG Y.K., LEE J.J., *Thin Solid Films*, 169 (1) (1989), 51.
- [2] BAGHER-MOHAGHEGHI M.M., SHOKOOH-SAREMI M., *J. Phys. D Appl. Phys.*, 37 (8) (2004), 1248.
- [3] JU S.Y., FACCHETTI A., XUAN, L. J., ISHIKAWA F., YE P.D., ZHOU C.W., MARKS T.J., JANES D.B., *Nat. Nanotechnol.*, 2 (6) (2007), 378.
- [4] HOSONO H., *Thin Solid Films*, 515 (15) (2007), 6000.
- [5] GRANQVIST C.G., *Sol. Energ. Mat. Sol. C*, 91 (17) (2007), 1529.
- [6] COUTTS T.J., YOUNG D.L., LI X., *Mater. Res. Bull.*, 25 (2000), 58.
- [7] ANSARI Z.A., ANSARI S.G., KO T., OH J.H., *Sensor. Actuat. B-Chem.*, 87 (1) (2002), 105.
- [8] HYODO T., ABE S., SHIMIZU Y., EGASHIRA M., *Sensor. Actuat. B-Chem.*, 93 (2003), 590.
- [9] GUZMAN G., DAHMANI B., PUETZ J., AEGERTER M.A., *Thin Solid Films*, 502 (1 – 2) (2006), 281.
- [10] NIRANJAN R.S., HWANG Y.K., KIM D.K., JHUNG S.H., CHANG J. S., MULLA I.S., *Mater. Chem. Phys.*, 92 (2 – 3) (2005), 384.
- [11] GRANQVIST C.G., *Thin Solid Films*, 193 – 194 (1990), 730.
- [12] LAMPERT C.M., *Sol. Energ. Mat. Sol. C*, 6 (1981), 1.
- [13] NANTO H., MINAMI T., TAKATA S., *J. Appl. Phys.*, 60 (2) (1986), 482.
- [14] ROZATI S.M., AKESTEH S., *Mater. Charact.*, 58 (4) (2007), 319.
- [15] SAKKA S., KOZUKA H., *Sol-Gel Processing*, Kluwer Academic, New York, 2005.
- [16] SINGH R., KUMAR M., SHANKAR S., SINGH R., GHOSH A.K., THAKUR O.P., DAS B., *Mat. Sci. Semi-con. Proc.*, 31 (2015), 310.

Received 2014-11-29

Accepted 2015-08-24